J Fluoresc (2017) 27:243–249
DOI 10.1007/s10895-016-1951-8

ORIGINAL ARTICLE

Disorder Amidst Membrane Order: Standardizing Laurdan Generalized Polarization and Membrane Fluidity Terms

Anthony G. Jay[1,2] **· James A. Hamilton**[1]

Received: 25 July 2016 / Accepted: 3 October 2016 / Published online: 13 October 2016

Abstract Membrane organization and fluidity research continues to expand and the understanding of membrane dynamics continues to be refined. Within this field of study, laurdan remains among the most popular, versatile, and established fluorescence probes. Fluorimetry and multiphoton microscopy techniques are standards for measuring laurdan fluorescence and continue to be refined. However, complications have arisen due to an amended membrane model, revised terms used for describing membrane phases, and wide variation in the selection of laurdan generalized polarization equation values. Here, in the context of the history and chemical properties of laurdan, discrepancies are highlighted and important recommendations are made to promote uniformity and ongoing progress.

Keywords Cholesterol · Fluorescence microscopy · Lipid rafts · Lipids · Membranes/fluidity · Phospholipids · Physical biochemistry

Abbreviations

LUT	Look-up table
DOPC	Dioleoyl phosphatidyl choline
SM	Sphingomyelin
Lo	Liquid ordered
Ld	Liquid disordered
SUV	Small unilamellar vesicle
LUV	Large unilamellar vesicle
GUV	Giant unilamellar vesicle
GPMV	Giant plasma membrane vesicles
FA	Fatty acid
GP	Generalized polarization
PM	Plasma membrane
RU	Relative units

✉ James A. Hamilton
jhamilt@bu.edu

[1] Department of Physiology & Biophysics, Boston University School of Medicine, Boston, MA 02118, USA

[2] Department of Biochemistry, Boston University School of Medicine, Boston, MA 02118, USA

Introduction

Over 40 fluorescence probes have been used to examine membrane properties, membrane domains, and membrane order [1]. Laurdan is one of the most established probes for studying overall membrane fluidity and its uses are rapidly expanding, from whole living zebrafish embryos down to single cell microdomain deconvolutions [2–4].

Following the synthesis and chemical characterization of prodan (6-propionyl-2-dimethylaminonaphthalene) in 1979 [5], which contained only a three fatty acid (FA) carbon tail, laurdan (6-dodecanoyl-2-dimethylaminonaphthalene) was developed soon after in 1981, with a twelve carbon FA tail. With this longer FA tail, laurdan maintains a more consistent membrane orientation and generally resides lower within the bilayer [6] (Fig. 1). Whereas prodan can probe the surface of a membrane, laurdan can probe both interfacial regions and the lipid bilayer close to the surface and is thus more versatile.

Since laurdan is incompatible with standard widefield and confocal fluorescence microscopy due to its low photostability, fluorescence spectroscopy has predominantly been in the past to monitor laurdan fluorescence. More recently, two-photon microscopy was demonstrated and endorsed for use with laurdan beginning in 1996 [9]. Since then, two-

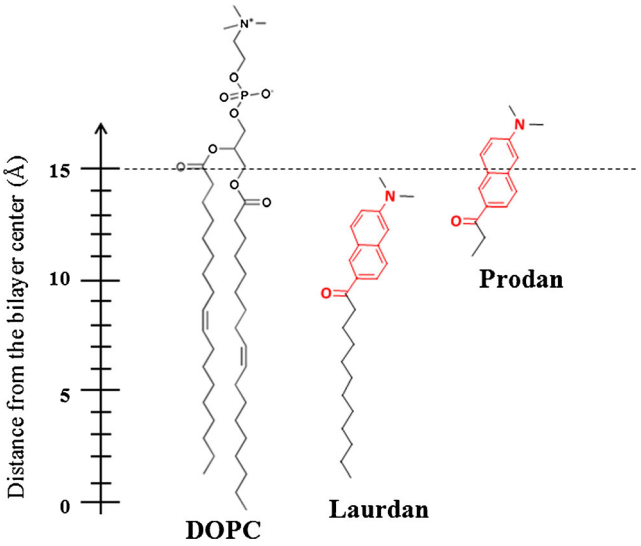

Fig. 1 Chemical structures of the phospholipid, dioleoyl phosphatidyl choline (DOPC) and laurdan and prodan, depicting their approximate bilayer locations, adapted from [7]. The phospholipid bilayer of live cells is normally 30–40 Å thick [8]

photon microscopy has grown into a common technique used to examine membrane organization with the laurdan probe, even while fluorimetry continues to be popular.

With both the two-photon microscopy and fluorimetry techniques, inconsistencies have become widespread in (i) describing membrane phase separated domains (gel, liquid crystalline, liquid ordered [Lo], liquid disordered [Ld], etc.), (ii) reporting membrane organization versus fluidity/order, and (iii) analyzing laurdan data from both two-photon microscopy and fluorescence spectroscopy. These will be discussed and clarified. Furthermore, specific suggestions will be offered to amend disparities.

Diverse Applications

Laurdan presents many merits for investigating membrane fluidity and has been used within an extensive range of membrane types: vesicles, supported bilayers, cells, organelles, and hybrid membrane systems. Applications include spectroscopic studies and microscopy imaging of phase separated domains as listed in Table 1. Inconsistencies of laurdan use have arisen at least in part from the diversity of these laurdan applications.

Early Lo and Ld Complications

The first characterizations of laurdan for detecting phospholipid membrane dynamics were performed in 1990. Herein, the concept of "generalized polarization" (GP) was introduced, which utilized the peak emission spectra wavelengths from the two pure lipid phases, gel (440 nm) and liquid crystalline (490 nm) [35].

A complication arose, beginning around 2001, when the classical fluid mosaic model of the membrane (including "gel" and "liquid crystalline" phase descriptions) was generally replaced by the view that the membrane was a complex combination of liquid ordered (Lo) and disordered (Ld) phases (reviewed and described here [1]). The Lo and Ld phases were defined as saturated and unsaturated membrane lipids, respectively, together with cholesterol. And while laurdan was among the first probes introduced for imaging Lo and Ld phases in model membranes [36], certain growing pains came with revising the long-standing fluid mosaic model. As a consequence, some publications that utilize laurdan to investigate membrane fluidity continue to include gel/crystalline (L_β and L_α, respectively) phase descriptions [20], or even a conglomeration of Lo, Ld, L_β, and L_α together [37]. Since typical studies using laurdan involve physiologically relevant conditions (*liquid* disordered or ordered; without freezing or boiling), we recommend that Lo and Ld be used in membrane phase descriptions involving laurdan (Fig. 2a).

Table 1 Fluidity studies using laurdan have been diverse. The uses of laurdan have included various liposomal vesicles, cell lines, and other membrane types

Liposomal Vesicles	Small Unilamellar Vesicles (SUVs) [10]
	Large Unilamellar Vesicles (LUVs) [11]
	Giant Unilamellar Vesicles (GUVs) [2]
	Vesicles Comprised Entirely of FA [12, 13]
Cell Lines	BY-2 tobacco cells [14], human macrophages and fibroblasts [15], MEF cells [16], MDCK and CV-1 cells [17], melanophore cells [18], neutrophils [19], OK kidney cells [20], oligodentrocytes [21], glioblastoma cells [22], *T. marmorata* cells [23], human spermatozoa cells [24], human endothelial cells [25], seven additional mammalian cell lines [26], assorted bacterial cells such as *G. stearothermophilus* [27] and *E. coli* [28], NIH3T3 cells [29], HeLa cells [4], HEK293 cells [4, 30]
Other Membrane Types	Native Pulmonary Surfactant [2, 31]
	Brain Cortex Membranes [32]
	Liver Microsomes [33]
	Giant Plasma Membrane Vesicles (GPMVs) [34]

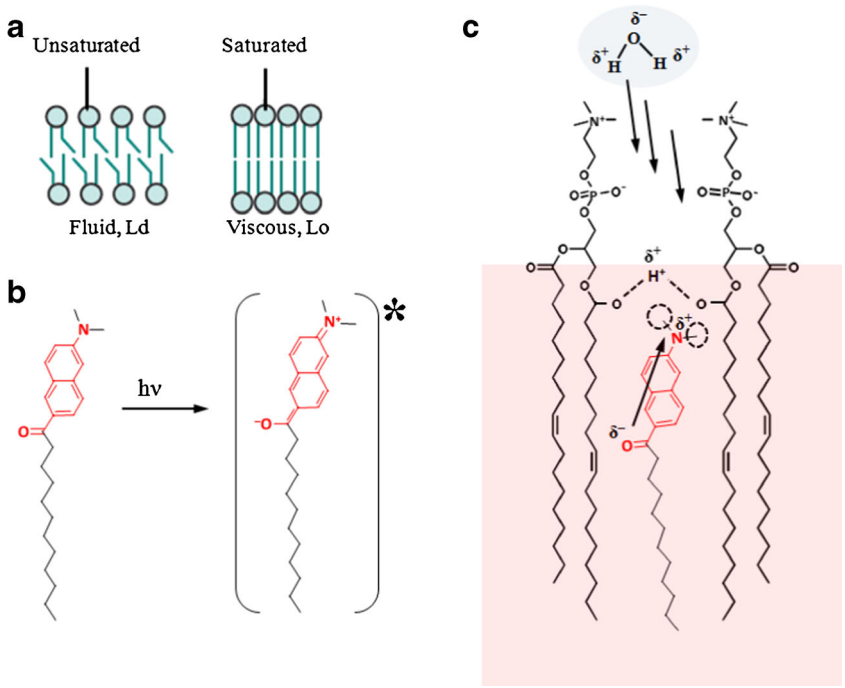

Fig. 2 **a** Schematic of an unsaturated Ld bilayer compared to a saturated Lo bilayer. **b** Structures of the ground and excited states of laurdan, where hν indicate the excitation. **c** Molecular model illustrating a representative "polarization-like state" of laurdan due to a weak interaction of the dimethylamino group of laurdan with the ester groups of DOPC. This interaction is strengthened by laurdan rising higher within the membrane (Ld phase) or interacting with certain other lipids such as sphingolipids (images modified from [3, 38])

Organization and Order

Due to continued advancements in two-photon microscopy with laurdan, Lo and Ld lipid phases are more readily visualized than ever before. Imaging now enables resolution to 200-300 nm and also allow user-defined domains or regions to be quantified using a simple and standardized laurdan macro readily compatible with Image J [4]. The visualization and quantification of membrane heterogeneity uses ratiometric changes in GP and nearly resolves individual microdomains 10-200 nm in size [39]. Due to these properties, laurdan has become a more a powerful tool for investigating everything from pathogens to healthy cells, or from toxic protein aggregates to normal proteins, or perturbations from exogenously added substances.

With these advances in imaging heterogeneity, a further clarification must be noted between membrane organization and fluidity/order. Historically, the term "fluidity" was used exclusively to describe biophysical membrane properties but "order" was later added (~1989) to precisely specify membrane organized domains [40]. With the revamped representation of membrane phases (liquid dis*ordered* and *ordered*), fluidity and order are now generally used synonymously [1] and organization (in place of "order") is currently being used to describe the organized domains (e.g. domains seen using laurdan with two-photon microscopy). While fluidity/order refer to overall Ld/Lo membrane phase ratios (as seen using fluorescence spectroscopy, for example), membrane organization refers to changes in phase location, density, and/or composition (in the case of introduced, membrane-embedded, substances) within the larger membrane context. Lipid organization, then, would be more readily observed from above a surface (X– or Y– plane) corresponding to lateral lipid packing, whereas lipid order or fluidity would normally be seen by a sample cross-section (Z– plane) or a full fluorimetry emission spectra. A publication by our group illustrates the new terminology in an application to lipid bilayers [41]. Another example of a recent application of the terms "organization" versus "fluidity/order" comes from an examination of oleic acid doses on membranes. This oleic acid study found that concentrations up to 100 μM had little effect on membrane fluidity but, at the same time, these concentrations inducted important changes in membrane lipid organization [42]. We recommend that similar precision is used with these terms, in ongoing and future laurdan research.

Environment Sensing

As a solvochromatic probe, laurdan that reports environmental changes through manifold properties. One way this occurs is through a progressive (non-binary) enhancement of laurdan charge separation within increasingly polar environments, which increases the dimethylamino dipole moment. Laurdan, therefore, has more than one excited state: a locally excited state intrinsic to the fluorophore and an internal charge transfer state created by the larger dipole moment [4] (Fig. 2b).

In addition to dipole-variable sensing of surroundings, a well-defined and unique property of the laurdan probe is its sensitivity to hydration levels [43]. Even while it is not fluorescent in a purely aqueous environment [44], laurdan shifts emission spectra when present in more or less hydrated

membrane environments due to H-bonding. This shift is significant, with several studies demonstrating that the water density at the location of laurdan is approximately 8 times higher in the Ld phase compared with the Lo phase [45, 46] (Fig. 2c). In the Ld phase, comprised mostly of unsaturated phosopholipid FA tails (containing more "kinks"), greater water penetration is permitted into the glycerol region of the bilayer surface and, as a consequence, the fluorescence spectra of laurdan exhibit a pronounced directional shift (a blueshift, in the case of the Ld phase, Fig. 2a and Fig. 3a). Importantly, these membrane-phase-dependent emission shifts have been reported as independent of the nature of the glycerophospholipid polar head group [48].

Miscellaneous accompanying properties further demonstrate why laurdan is a popular and prominent probe for use in membrane dynamics studies. Laurdan has been found to maintain no preferential orientation within Ld membranes, but is present in a constrained vertical orientation in Lo membranes. This orientation further boosts emission shift changes that are already present from hydration and/or polar-environment dipole separations [49] (detailed orientation characterizations also here [50]). Moreover, while the C-laurdan analogue gives higher fluorescence quantum yields within the Lo phase [1] and prodan preferentially partitions to the Lo phase of a membrane [51], laurdan partitions equally between Lo and Ld and gives comparable quantum yields in both phases [52]. Hence, among membrane localized fluorescence probes, laurdan offers minimal negative characteristics while multiplying and enhancing environmental change-detection through several characteristics: polarity-dependent charge separation, the strength of available H-bonding interactions, hydration sensitivity, and lateral molecular constraint/freedom [53, 54].

Redshift, Blueshift

In the early characterizations of laurdan described above, environment-dependent fluorescence emission spectra shifts were quantified using those values (440/490 nm) that represented the peak positions reached in the two pure lipid phases [26, 35]. Included in these characterizations, traditional terminology was borrowed from physics to describe the *direction* of a laurdan spectrum shift as a "redshift", indicating an increase in a peak spectrum wavelength (when comparing two conditions), or a "blueshift", indicating a decrease in wavelength. This led to the important and widely used excitation generalized polarization (exGP) equation: $exGP = I_B - I_R / I_B + I_R$ where I = intensity, B = blue (440 nm), and R = red (490 nm) (Fig. 3a).

The exGP equation has become nearly ubiquitous for quantifying and comparing laurdan spectra replicates and differing experimental conditions. However, GP_{Red} is intuitively confusing since the 490 nm wavelength is tangibly green within the visible spectrum. Subsequently, a few recent studies use GP_{Green} rather than GP_{Red} (as in: $exGP = I_B - I_G / I_B + I_G$) [45]

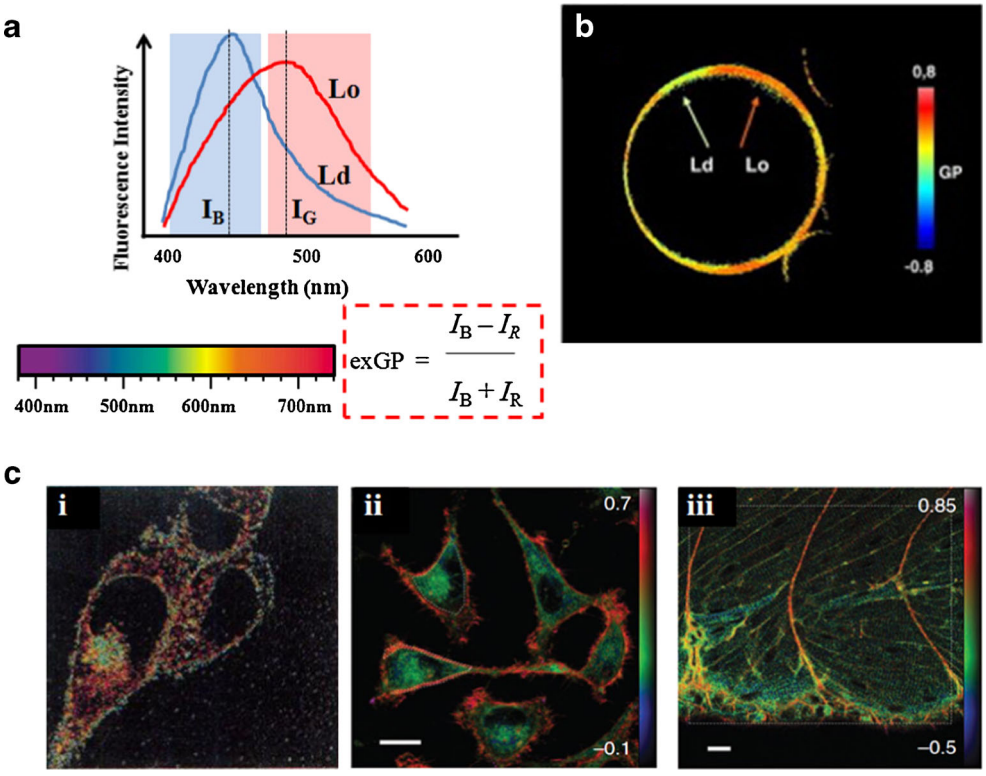

Fig. 3 **a** Schematic of two separate laurdan fluorescence emission spectra (*blue* and *red lines*), illustrating a blue shift or a red shift which occur within Ld or Lo phases, respectively. Below are the visible spectrum wavelengths and corresponding wavelength colors (adopted from [47]), as well as the generic ratiometric exGP equation. **b** Laurdan ratiometric (GP) microscopy image of a GUV (SM/DOPC/cholesterol mixture) containing laurdan, with arrows illustrating Ld and Lo phases and including a standard colorimetric GP-LUT bar (modified from [2]). **c** The (i) first published laurdan 2-photon microscopy image of live MEF cells, compared to a (ii) recent 2-photon microscopy image of live HEK293 cells and (iii) a live, 5-d-old zebrafish embryo muscle tissue (10 μM scale bars) containing laurdan (images modified from [4, 9])

even while the majority of current publications continue to use GP_{Red}. This semantic confusion is understandable because (i) redshift terminology is imprecise albeit historical, and (ii) the laurdan shift is not actually within the red wavelengths, but rather *toward* the red direction, since red is at the far end of the ROYGBIV visible spectrum (~700 nm). Compounding the confusion, GP_{Blue} (from "blueshift") is always used in laurdan literature rather than "GP_{Violet}", which would be at the opposite end of the visible spectrum from red. Further, the GP_{Blue} 440 nm value coincidentally is authentically blue within the visible light spectrum (Fig. 3a). Therefore and in this case, the exact visible spectrum color is used (blue) rather than merely the true *direction* of the visible spectrum color shift (violet).

Despite the logical validity of using GP_{Green} to describe the laurdan emission Lo phase shift, the redshift/blueshift and corresponding GP_{Red}/GP_{Blue} is recommended for use since the vast majority of literature up to and including current work continues to use GP_{Red}/GP_{Blue}. Additionally, the redshift/blueshift terms have expanded within physics and biophysics to include wavelengths far outside the visible spectra (such as gamma rays ([55]) or microwaves [56] etc.), which indicates that these terms will continue to be used to describe *directional* shifts. Finally, colorimetric look-up tables (LUTs) are often inserted into laurdan two-photon microscopy images and represent increased membrane order (up to red) and decreased order (down to blue) based on the corresponding GP values and ranging from −1.0 to +1.0 (Fig. 3b). Even while these LUTs are assigned arbitrary representative colors and, as such, are not actual representations of the visible spectrum, red has been chosen to represent the +1.0 end, while blue has been assigned to the −1.0 end of the standard GP LUT. If the Lo phase was described as a green shift, these modified LUTs would likely create confusion.

Generalized Polarization Discrepancies

Since the redshift and blueshift GP equation terms have been inconsistent within published literature, it is not surprising that wide variability also exists in numerical fluorescence *spectroscopy* exGP values as well as in two-photon *microscopy* emission input values (where dual emission *ranges* must be manually selected in microscopy software that represent Ld and Lo phases).

For example, two-photon microscopy uses the ratiometric equation: $GP = I_B - I_R / I_B + I_R$, and some groups use the values I_B = 400-460 nm and I_R = 470-530 nm [4], others use I_B = 410-490 nm and I_R = 503-553 nm [25]; others I_B = 420-460 nm and I_R = 470-510 nm [34]; or I_B = 415-455 nm and I_R = 490-530 nm [18]; or I_B = 395-455 nm and I_R = 470-550 nm [19]; or I_B = 460-480 nm and I_R = 540-550 nm [29]; or I_B = 430-440 nm and I_R = 480-500 nm [20]; or I_B = 410-470 nm and I_R = 500-536 nm [21]. This variability between publications inevitably leads to variability within results between groups and difficulty comparing them, even when the same cell types or model membranes are used.

Furthermore, other aspects of laurdan two-photon data analysis lack congruity. This is normally subtler and less problematic than GP range values, since many different membranes are investigated and specific modes of analysis are required. Most studies use their version of the GP equation to analyze the data and either choose a specific region to quantify (e.g. within a cell [25]) or manually outline and distinguish between the inner and outer regions (the PM versus the intracellular space, for example [4]). Using a free custom-written macro with Image J software (NIH, Bethesda), this process has recently been standardized and simplified using the following GP values: I_B = 400-460 nm and I_R = 470-530 nm [4]. Since these values are also the most widely published for laurdan and two-photon microscopy, these are recommended for use in order to standardize this area of study.

In fluorimetry spectroscopy studies using laurdan, significant variation once again exists with exGP values (even while I_B and I_R are *single* numerical values and not a range of values, as in two-photon microscopy). Using the standard equation: $exGP = I_B - I_R / I_B + I_R$, many studies use the original I_B = 440 and I_R = 490 [10–12, 17, 27, 28, 32, 57–59]; others use I_B = 435 and I_R = 490 [33]; or I_B = 435 and I_R = 480 [60]; or I_B = 430 and I_R = 500 [13]; or I_B = 430 and I_R = 480 [24]; or I_B = 434 and I_R = 490 [23]; or I_B = 430 and I_R = 490 [14]. Additional procedures to analyze laurdan emission spectra have been developed that rely on the log-normal asymmetric function rather than Gaussian distributions [45], and we believe that either these new tools should be used, or the original 440/490 values exactly, to maintain consistency and comparison among laurdan spectroscopic studies.

Summary and Conclusions

Added to cells, model membranes, or even live organisms, the single probe laurdan has been shown to (i) distinguish Lo and Ld organized domains, (ii) sense PM phospholipid bilayer fluidity, and (iii) sense intracellular fluidity, all with relatively easy experimental methods, fast response times, and high spatial resolutions. While many fluorescence probes work extremely well in model lipid membranes, only a few function as predicted/expected within live cells [1]. Laurdan is an example that works well in live cells, making it a more important probe than ever. This review delineates the deviations within membrane phase terminology (and recommends Ld/Lo), membrane phase descriptions (and recommends fluidity/order versus organization), GP equation terms (and recommends redshift/blueshift [I_B and I_R] terms), exGP fluorimetry values (and recommends I_B = 440 and I_R = 490), and GP two-photon microscopy range values (and recommends I_B = 400-

460 nm and I_R = 470-530 nm). These propositions might not only contribute to the expanding field of study using laurdan, but may benefit the growing library of laurdan analogues (2,6 substituted naphthalene derivatives) such as C-laurdan, patman, prodan, acdan, danca, and acrylodan, that often adapt laurdan data analysis strategies and equations [4, 18, 48].

References

1. Klymchenko AS, Kreder R (2014) Fluorescent probes for lipid rafts: from model membranes to living cells. Chem Biol 21:97–113
2. Bagatolli LA (2006) To see or not to see: lateral organization of biological membranes and fluorescence microscopy. Biochim Biophys Acta 1758:1541–1556
3. Gaus K, Zech T, Harder T (2006) Visualizing membrane microdomains by laurdan 2-photon microscopy. Mol Membr Biol 23:41–48
4. Owen DM, Rentero C, Magenau A, Abu-Siniyeh A, Gaus K (2012) Quantitative imaging of membrane lipid order in cells and organisms. Nat Protoc 7:24–35
5. Weber G, Farris FJ (1979) Synthesis and spectral properties of a hydrophobic fluorescent probe: 6-propionyl-2-(dimethylamino)naphthalene. Biochemistry 18:3075–3078
6. MacGregor, R., and Weber, G. (1981) Fluorophores in polar media: spectral effects of the Langevin distribution of electrostatic interactions. Ann NY Acad Sci 140–154
7. Jurkiewicz P, Cwiklik L, Jungwirth P, Hof M (2012) Lipid hydration and mobility: an interplay between fluorescence solvent relaxation experiments and molecular dynamics simulations. Biochimie 94:26–32
8. Mitra K, Ubarretxena-Belandia I, Taguchi T, Warren G, Engelman DM (2004) Modulation of the bilayer thickness of exocytic pathway membranes by membrane proteins rather than cholesterol. Proc Natl Acad Sci U S A 101:4083–4088
9. Yu W, So PT, French T, Gratton E (1996) Fluorescence generalized polarization of cell membranes: a two-photon scanning microscopy approach. Biophys J 70:626–636
10. Sotomayor CP, Aguilar LF, Cuevas FJ, Helms MK, Jameson DM (2000) Modulation of pig kidney Na+/K + −ATPase activity by cholesterol: role of hydration. Biochemistry 39:10928–10935
11. Samuni AM, Lipman A, Barenholz Y (2000) Damage to liposomal lipids: protection by antioxidants and cholesterol-mediated dehydration. Chem Phys Lipids 105:121–134
12. Suga K, Yokoi T, Kondo D, Hayashi K, Morita S, Okamoto Y, Shimanouchi T, Umakoshi H (2014) Systematical characterization of phase behaviors and membrane properties of fatty acid/didecyldimethylammonium bromide vesicles. Langmuir: the ACS journal of surfaces and colloids 30:12721–12728
13. Budin I, Debnath A, Szostak JW (2012) Concentration-driven growth of model protocell membranes. J Am Chem Soc 134:20812–20819
14. Roche Y, Klymchenko AS, Gerbeau-Pissot P, Gervais P, Mely Y, Simon-Plas F, Perrier-Cornet JM (2010) Behavior of plant plasma membranes under hydrostatic pressure as monitored by fluorescent environment-sensitive probes. Biochim Biophys Acta 1798:1601–1607
15. Gaus K, Gratton E, Kable EP, Jones AS, Gelissen I, Kritharides L, Jessup W (2003) Visualizing lipid structure and raft domains in living cells with two-photon microscopy. Proc Natl Acad Sci U S A 100:15554–15559
16. Le Lay S, Li Q, Proschogo N, Rodriguez M, Gunaratnam K, Cartland S, Rentero C, Jessup W, Mitchell T, Gaus K (2009) Caveolin-1-dependent and -independent membrane domains. J Lipid Res 50:1609–1620
17. Mamdouh Z, Giocondi MC, Le Grimellec C (1998) In situ determination of intracellular membrane physical state heterogeneity in renal epithelial cells using fluorescence ratio microscopy. Eur Biophys J 27:341–351
18. Dodes Traian MM, Gonzalez Flecha FL, Levi V (2012) Imaging lipid lateral organization in membranes with C-laurdan in a confocal microscope. J Lipid Res 53:609–616
19. Sitrin RG, Sassanella TM, Landers JJ, Petty HR (2010) Migrating human neutrophils exhibit dynamic spatiotemporal variation in membrane lipid organization. Am J Respir Cell Mol Biol 43:498–506
20. Kovacs E, Savopol T, Iordache MM, Saplacan L, Sobaru I, Istrate C, Mingeot-Leclercq MP, Moisescu MG (2012) Interaction of gentamicin polycation with model and cell membranes. Bioelectrochemistry 87:230–235
21. Kahn E, Baarine M, Dauphin A, Ragot K, Tissot N, Seguin A, Menetrier F, Kattan Z, Bachelet CM, Frouin F, Lizard G (2011) Impact of 7-ketocholesterol and very long chain fatty acids on oligodendrocyte lipid membrane organization: evaluation via LAURDAN and FAMIS spectral image analysis. Cytometry Part A: the journal of the International Society for Analytical Cytology 79:293–305
22. Weber P, Wagner M, Schneckenburger H (2010) Fluorescence imaging of membrane dynamics in living cells. J Biomed Opt 15:046017
23. Antollini SS, Barrantes FJ (2002) Unique effects of different fatty acid species on the physical properties of the torpedo acetylcholine receptor membrane. J Biol Chem 277:1249–1254
24. Buffone MG, Doncel GF, Calamera JC, Verstraeten SV (2009) Capacitation-associated changes in membrane fluidity in asthenozoospermic human spermatozoa. Int J Androl 32:360–375
25. Shentu TP, Titushkin I, Singh DK, Gooch KJ, Subbaiah PV, Cho M, Levitan I (2010) oxLDL-induced decrease in lipid order of membrane domains is inversely correlated with endothelial stiffness and network formation. Am J Physiol Cell Physiol 299:C218–C229
26. Parasassi T, Loiero M, Raimondi M, Ravagnan G, Gratton E (1993) Absence of lipid gel-phase domains in seven mammalian cell lines and in four primary cell types. Biochim Biophys Acta 1153:143–154
27. Georget E, Kapoor S, Winter R, Reineke K, Song Y, Callanan M, Ananta E, Heinz V, Mathys A (2014) In situ investigation of Geobacillus stearothermophilus spore germination and inactivation mechanisms under moderate high pressure. Food Microbiol 41:8–18
28. Simonin H, Bergaoui IM, Perrier-Cornet JM, Gervais P (2014) Cryopreservation of *Escherichia coli* K12TG1: protection from the damaging effects of supercooling by freezing. Cryobiology 70(2):115–121
29. Golfetto O, Hinde E, Gratton E (2013) Laurdan fluorescence lifetime discriminates cholesterol content from changes in fluidity in living cell membranes. Biophys J 104:1238–1247
30. Brejchova J, Sykora J, Dlouha K, Roubalova L, Ostasov P, Vosahlikova M, Hof M, Svoboda P (2011) Fluorescence spectroscopy studies of HEK293 cells expressing DOR-Gi1alpha fusion protein; the effect of cholesterol depletion. Biochim Biophys Acta 1808:2819–2829
31. Parasassi T, Gratton E, Yu WM, Wilson P, Levi M (1997) Two-photon fluorescence microscopy of laurdan generalized polarization domains in model and natural membranes. Biophys J 72:2413–2429
32. Sykora J, Bourova L, Hof M, Svoboda P (2009) The effect of detergents on trimeric G-protein activity in isolated plasma membranes from rat brain cortex: correlation with studies of DPH and laurdan fluorescence. Biochim Biophys Acta 1788:324–332

33. Garda HA, Bernasconi AM, Brenner RR, Aguilar F, Soto MA, Sotomayor CP (1997) Effect of polyunsaturated fatty acid deficiency on dipole relaxation in the membrane interface of rat liver microsomes. Biochim Biophys Acta 1323:97–104
34. Sezgin E, Kaiser HJ, Baumgart T, Schwille P, Simons K, Levental I (2012) Elucidating membrane structure and protein behavior using giant plasma membrane vesicles. Nat Protoc 7:1042–1051
35. Parasassi T, De Stasio G, d'Ubaldo A, Gratton E (1990) Phase fluctuation in phospholipid membranes revealed by laurdan fluorescence. Biophys J 57:1179–1186
36. Dietrich C, Bagatolli LA, Volovyk ZN, Thompson NL, Levi M, Jacobson K, Gratton E (2001) Lipid rafts reconstituted in model membranes. Biophys J 80:1417–1428
37. M'Baye G, Mely Y, Duportail G, Klymchenko AS (2008) Liquid ordered and gel phases of lipid bilayers: fluorescent probes reveal close fluidity but different hydration. Biophys J 95:1217–1225
38. Bagatolli LA, Parasassi T, Fidelio GD, Gratton E (1999) A model for the interaction of 6-lauroyl-2-(N,N-dimethylamino)naphthalene with lipid environments: implications for spectral properties. Photochem Photobiol 70:557–564
39. Owen DM, Gaus K (2013) Imaging lipid domains in cell membranes: the advent of super-resolution fluorescence microscopy. Front Plant Sci 4:503
40. van Ginkel G, van Langen H, Levine YK (1989) The membrane fluidity concept revisited by polarized fluorescence spectroscopy on different model membranes containing unsaturated lipids and sterols. Biochimie 71:23–32
41. Guo W, Kurze V, Huber T, Afdhal NH, Beyer K, Hamilton JA (2002) A solid-state NMR study of phospholipid-cholesterol interactions: sphingomyelin-cholesterol binary systems. Biophys J 83: 1465–1478
42. Yang Q, Alemany R, Casas J, Kitajka K, Lanier SM, Escriba PV (2005) Influence of the membrane lipid structure on signal processing via G protein-coupled receptors. Mol Pharmacol 68:210–217
43. Parasassi T, Krasnowska E, Bagatolli L, Gratton E (1998) Laurdan and prodan as polarity-sensitive fluorescent membrane probes. J Fluoresc 8(4):365–373
44. Parasassi T, Giusti AM, Gratton E, Monaco E, Raimondi M, Ravagnan G, Sapora O (1994) Evidence for an increase in water concentration in bilayers after oxidative damage of phospholipids induced by ionizing radiation. Int J Radiat Biol 65:329–334
45. Bacalum M, Zorila B, Radu M (2013) Fluorescence spectra decomposition by asymmetric functions: laurdan spectrum revisited. Anal Biochem 440:123–129
46. Stepniewski M, Bunker A, Pasenkiewicz-Gierula M, Karttunen M, Rog T (2010) Effects of the lipid bilayer phase state on the water membrane interface. J Phys Chem B 114:11784–11792
47. Pasachoff J, Filippenko A (2007) The cosmos: astronomy in the new millennium. Thompson Higher Education, 3rd Ed. Brooks/ Cole Publishing, p 480
48. Mély Y, Duportail G, Bagatolli LA (2013) Fluorescent methods to study biological membranes. Springer, Heidelberg, New York
49. Demchenko AP, Mely Y, Duportail G, Klymchenko AS (2009) Monitoring biophysical properties of lipid membranes by environment-sensitive fluorescent probes. Biophys J 96:3461–3470
50. Parisio G, Marini A, Biancardi A, Ferrarini A, Mennucci B (2011) Polarity-sensitive fluorescent probes in lipid bilayers: bridging spectroscopic behavior and microenvironment properties. J Phys Chem B 115:9980–9989
51. Kaiser HJ, Lingwood D, Levental I, Sampaio JL, Kalvodova L, Rajendran L, Simons K (2009) Order of lipid phases in model and plasma membranes. Proc Natl Acad Sci U S A 106:16645–16650
52. Krasnowska EK, Gratton E, Parasassi T (1998) Prodan as a membrane surface fluorescence probe: partitioning between water and phospholipid phases. Biophys J 74:1984–1993
53. Catalan J, Perez P, Laynez J, Blanco FG (1991) Analysis of the solvent effect on the photophysics properties of 6-propionyl-2-(dimethylamino)naphthalene (PRODAN). J Fluoresc 1:215–223
54. Cerezo F, Rocafort SC, Sierra PS, Garcia-Blanco F, Oliva CD, Sierra JC (2001) Photophysical study of the probes acrylodan (1-[6-(dimethylamino)naphthalen-2-yl]prop-2-en-1-one), ANS (8-anilinonaphthalene- 1-sulfonate) and prodan (1-[6-(dimethylamino)naphthalen- 2-yl]propan-1-1) in aqueous mixtures of various alcohols. Helv Chim Acta 84:3306–3312
55. Tagliaferri G, Salvaterra R, Campana S, Covino S, D'Avanzo P, Fugazza D, Ghirlanda G, Ghisellini G, Melandri A, Nava L, Sbarufatti B, Vergani S (2013) A complete sample of long bright Swift gamma ray bursts. Philosophical transactions Series A, Mathematical, physical, and engineering sciences 371:20120235
56. Kang L, Zhao Q, Zhao H, Zhou J (2008) Magnetically tunable negative permeability metamaterial composed by split ring resonators and ferrite rods. Opt Express 16:8825–8834
57. Kastorna A, Trusova V, Gorbenko G, Kinnunen P (2012) Membrane effects of lysozyme amyloid fibrils. Chem Phys Lipids 165:331–337
58. Maitani Y, Nakamura A, Tanaka T, Aso Y (2012) Hydration of surfactant-modified and PEGylated cationic cholesterol-based liposomes and corresponding lipoplexes by monitoring a fluorescent probe and the dielectric relaxation time. Int J Pharm 427:372–378
59. Luciani P, Bombelli C, Colone M, Giansanti L, Ryhanen SJ, Saily VM, Mancini G, Kinnunen PK (2007) Influence of the spacer of cationic gemini amphiphiles on the hydration of lipoplexes. Biomacromolecules 8:1999–2003
60. Soderlund T, Alakoskela JM, Pakkanen AL, Kinnunen PK (2003) Comparison of the effects of surface tension and osmotic pressure on the interfacial hydration of a fluid phospholipid bilayer. Biophys J 85:2333–2341